

## NMR Structure and Dynamic Studies of an Anion-Binding, Channel-Forming Heptapeptide

Gabriel A. Cook,<sup>†</sup> Robert Pajewski,<sup>||</sup> Mahalaxmi Aburi,<sup>†</sup> Paul E. Smith,<sup>‡</sup>  
Om Prakash,<sup>†</sup> John M. Tomich,<sup>†</sup> and George W. Gokel<sup>\*,§,||</sup>

Contribution from the Departments of Biochemistry and Chemistry, Kansas State University, Manhattan, Kansas 66506, Department of Chemistry, Washington University, 1 Brookings Drive, St. Louis, Missouri 63130, and Department of Molecular Biology & Pharmacology, Washington University School of Medicine, Campus Box 8103, 660 S. Euclid Avenue, St. Louis, Missouri 63110

Received September 6, 2005; E-mail: ggokel@wustl.edu

**Abstract:** The synthetic peptide (C<sub>18</sub>H<sub>37</sub>)<sub>2</sub>NCOCH<sub>2</sub>OCH<sub>2</sub>CON-(Gly)<sub>3</sub>-Pro-(Gly)<sub>3</sub>-OCH<sub>2</sub>Ph forms chloride-selective channels in liposomes and exhibits voltage-gating properties in planar phospholipid bilayers. The peptide fragment of the channel is based on a conserved motif in naturally occurring chloride transporters. Membrane-anchoring residues at the N- and C-terminal ends augment the peptide. NMR spectra (1D and 2D) of the channel in CDCl<sub>3</sub> showed significant variation in the absence and presence of stoichiometric tetrabutylammonium chloride (Bu<sub>4</sub>NCl). One-dimensional solution-state NMR titration studies combined with computational molecular simulation studies indicate that the peptide interacts with the salt as an ion pair and H-bonds chloride. To our knowledge, this is the first structural analysis of any synthetic anion-channel salt complex.

### Introduction

The remarkable structural and mechanistic complexity exhibited by natural ion-conducting channels has led to the design of several synthetic model systems.<sup>1–3</sup> This includes de novo designed systems<sup>4</sup> and truncated or otherwise modified natural peptide sequences.<sup>5,6</sup> A number of compounds have been designed to function as chloride transporters in phospholipid bilayers for the purpose of studying the chemistry and biophysics of pore formation.<sup>7</sup> The subject of the present work is a heptapeptide having the structure (C<sub>18</sub>H<sub>37</sub>)<sub>2</sub>N-COCH<sub>2</sub>OCH<sub>2</sub>-CON-(Gly)<sub>3</sub>-Pro-(Gly)<sub>3</sub>-OCH<sub>2</sub>Ph (**1**).<sup>8</sup> It was designed on the basis of naturally occurring chloride transporters that have a conserved GxxP motif. Three glycine residues flank proline in **1**. This conforms to the GxxP sequence requirement and affords synthetic simplicity. Proline is present in the anion pathway of all known chloride channels. Indeed, when proline is substituted into the selectivity filter of the nicotinic acetylcholine receptor, the selectivity changes from cation to anion.<sup>9,10</sup>

Proline's cyclic structure has also been shown to be important for the "hinge bend" of other channel-forming peptides.<sup>11</sup> When proline in **1** is replaced by its six-membered-ring analogue, pipercolic acid, the activity and selectivity are dramatically reduced.<sup>12,13</sup> A N-terminal, dialkylamino group was linked to the heptapeptide through diglycolic acid. In combination, these residues mimic the fatty acid chains of natural phospholipids in size, polarity, and functional group position. The C-terminal benzyl group was incorporated to reduce the carboxyl group's polarity (charge), but extensive structural studies<sup>14</sup> have shown that the ester residue also serves as a secondary anchor. It is believed that the heptapeptide resides at the membrane-water interface and forms an uncharged, chloride-selective portal that is held at the membrane surface by the hydrophobic anchor. The aqueous pathway created by this structure, if maintained long enough, can allow diffusion of chloride to the interior of the bilayer.

Several lines of evidence suggest that **1** functions as a dimer. For example, analogues of **1** in which the compounds were linked at either their C- or N-terminal sides transported chloride through liposomal bilayers faster than twice the concentration of **1**.<sup>15</sup> Whatever the precise nature of the pore, planar bilayer

<sup>†</sup> Department of Biochemistry, Kansas State University.

<sup>‡</sup> Department of Chemistry, Kansas State University.

<sup>§</sup> Department of Chemistry, Washington University.

<sup>||</sup> Department of Molecular Biology & Pharmacology, Washington University School of Medicine.

(1) Gokel, G. W.; Murillo, O. *Acc. Chem. Res.* **1996**, *29*, 425–432.

(2) Gokel, G. W. *Chem. Commun.* **2000**, 1–9.

(3) Gokel, G. W.; Mukhopadhyay, A. *Chem. Soc. Rev.* **2001**, *30*, 274–286.

(4) Åkerfeldt, K. S.; Lear, J. D.; Wasserman, Z. R.; Chung, L. A.; DeGrado, W. F. *Acc. Chem. Res.* **1993**, *26*, 191–197.

(5) Wallace, D. P.; Tomich, J. M.; Iwamoto, T.; Henderson, K.; Grantham, J. J.; Sullivan, L. P. *Am. J. Physiol.* **1997**, *272*, C1672–C1679.

(6) Wallace, D. P.; Tomich, J. M.; Eppler, J. W.; Iwamoto, T.; Grantham, J. J.; Sullivan, L. P. *Biochim. Biophys. Acta* **2000**, *1464*, 69–82.

(7) Oblatt-Montal, M.; Buhler, L. K.; Iwamoto, T.; Tomich, J. M.; Montal, M. *J. Biol. Chem.* **1993**, *268*, 14601–7.

(8) Schlesinger, P. H.; Ferdani, R.; Liu, J.; Pajewska, J.; Pajewski, R.; Saito, M.; Shabany, H.; Gokel, G. W. *J. Am. Chem. Soc.* **2002**, *124*, 1848–9.

(9) Galzi, J. L.; Devillers-Thiery, A.; Hussy, N.; Bertrand, S.; Changeux, J. P.; Bertrand, D. *Nature* **1992**, *359*, 500–505.

(10) Corring, P. J.; Bertrand, S.; Galzi, J.; Devillers-Thiery, A.; Changeux, J.-P.; Bertrand, D. *Neuron* **1999**, *22*, 831–843.

(11) Gibbs, N.; Sessions, R. B.; Williams, P. B.; Dempsey, C. E. *Biophys. J.* **1997**, *72*, 2490–2495.

(12) Schlesinger, P. H.; Ferdani, R.; Pajewska, J.; Pajewski, R.; Gokel, G. W. *New J. Chem.* **2003**, *27*, 60–67.

(13) Ferdani, R.; Pajewski, R.; Djedovic, N.; Pajewska, J.; Schlesinger, P. H.; Gokel, G. W. *New J. Chem.* **2005**, *29*, 673–680.

(14) Djedovic, N.; Ferdani, R.; Harder, E.; Pajewska, J.; Pajewski, R.; Schlesinger, P. H.; Gokel, G. W. *Chem. Commun.* **2003**, 2862–3.

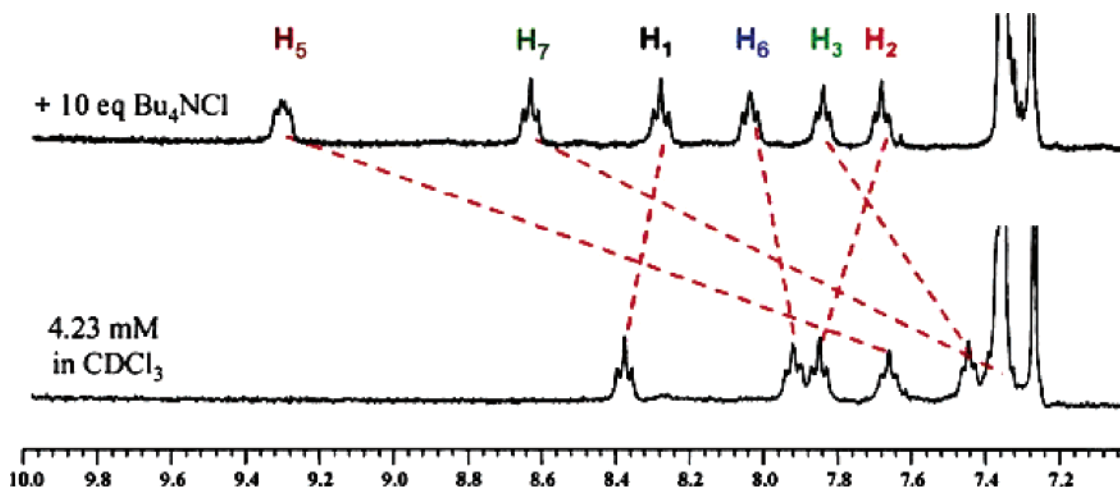
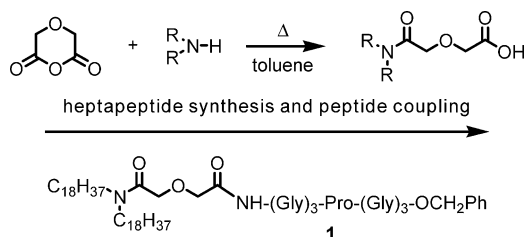


**Figure 1.** One-dimensional  $^1\text{H}$  NMR spectra of **1** ( $\text{CDCl}_3$ ,  $25^\circ\text{C}$ ). The  $^1\text{H}$  NMR spectra show resonances of **1** in the absence of  $\text{Bu}_4\text{NCl}$  (bottom) and in the presence of 10 equiv of  $\text{Bu}_4\text{NCl}$  (top).

#### Scheme 1



voltage clamp experiments clearly showed that **1** exhibits open-close channel behavior and voltage-dependent gating in planar phospholipid bilayers.<sup>8</sup>

In the work reported here, the structure of **1** in  $\text{CDCl}_3$  solution has been determined by  $^1\text{H}$  NMR spectroscopy in the presence and absence of  $\text{Bu}_4\text{NCl}$ . The conformation of **1** is significantly different in the presence of salt, and the NMR results are in accord with previous ion-pair complexation studies.<sup>16</sup>

## Results and Discussion

**Preparation of the Required Compounds.** The preparation of **1** has been reported in detail.<sup>17</sup> Briefly, dioctadecylamine is heated in toluene with diglycolic anhydride to give, after evaporation of solvent and crystallization,  $(\text{C}_{18}\text{H}_{37})_2\text{N}-\text{COCH}_2\text{OCH}_2\text{COOH}$ . The heptapeptide is made by standard coupling methods. The diglycolic acid derivative is formally coupled to  $\text{H}_2\text{N}-(\text{Gly})_3-\text{Pro}-(\text{Gly})_3-\text{OCH}_2\text{Ph}$  to give  $(\text{C}_{18}\text{H}_{37})_2\text{N}-\text{COCH}_2\text{OCH}_2\text{CON}-(\text{Gly})_3-\text{Pro}-(\text{Gly})_3-\text{OCH}_2\text{Ph}$  (**1**). The preparation is summarized in Scheme 1.

To distinguish the NMR signals arising from the six glycine residues, six analogues of **1** were prepared in which a deuterioglycine replaced the respective amino acid at each position. The assignments made here were made unequivocally based on the individual deuterated compounds (reported elsewhere<sup>18</sup>). The glycine amide protons are designated  $^1\text{G}_{\text{NH}}$  to  $^7\text{G}_{\text{NH}}$  from the N-terminal to the C-terminal end of the heptapeptide. No amide proton is present on proline.

**Table 1.**  $^1\text{H}$  NMR Chemical Shifts for **1** in the Absence and Presence of  $\text{Bu}_4\text{NCl}$  in  $\text{CDCl}_3$

residue	free	+ salt <sup>a</sup>	$\Delta\delta^b$
Gly-1	8.37	8.27	0.10
Gly-2	7.85	7.68	0.17
Gly-3	7.45	7.84	-0.39
Gly-5	7.66	9.30	-1.64
Gly-6	7.92	8.03	-0.11
Gly-7	7.34	8.63	-1.29

<sup>a</sup> Addition of 10 equiv of  $\text{Bu}_4\text{NCl}$ . <sup>b</sup> Chemical shift difference  $\delta_{\text{free}} - \delta_{\text{salt}}$ .

**NMR Analysis of **1** in  $\text{CDCl}_3$ .** One-dimensional  $^1\text{H}$  NMR studies revealed chemical shift changes for all of the amide protons in **1** when the peptide sample was titrated with  $\text{Bu}_4\text{NCl}$ . Figure 1 shows the spectrum of **1** (4.23 mM in  $\text{CDCl}_3$ , bottom trace). Several of the amide NH chemical shifts are significantly altered in the presence of  $\text{Bu}_4\text{NCl}$ , suggesting direct H-bond interactions with the chloride anion.

One- and two-dimensional  $^1\text{H}-^1\text{H}$  NMR experiments were conducted on **1** in the absence and presence of  $\text{Bu}_4\text{NCl}$ . The numerous differences are apparent in Figure 1. Sequential assignments based on analysis of  $^1\text{H}-^1\text{H}$  NOESY spectra [ $\text{C}_{\alpha\text{H}}(i)$  to  $\text{NH}(i+1)$ ] were used to interpret the spectra. Fortunately, the amide resonances of all six glycines were well separated in both cases.

Chemical shift changes experienced when **1** was in the absence or presence of  $\text{Bu}_4\text{NCl}$  (10 equiv,  $\text{CDCl}_3$ ,  $25^\circ\text{C}$ ) are recorded in Table 1. The largest difference in chemical shift was that of the  $^5\text{G}_{\text{NH}}$  amide proton, which moved downfield by 1.64 ppm. These differences are thought to result from structural changes in the peptide caused by an ion-pair interaction. The large shift of  $^5\text{G}_{\text{NH}}$  suggests that it might interact strongly with the chloride anion.

Further analysis of changes in peptide secondary structure was accomplished by conducting TOCSY and NOESY experiments. NOESY spectral analysis showed sequential ( $i$  to  $i+1$ ) medium ( $i$  to  $\geq i+2$  and  $< i+4$ ) and long-range ( $i$  to  $\geq i+4$ ) NH-NH NOE cross-peaks. In the amide region, there were sequential NH-NH connectivities from  $^1\text{G}_{\text{NH}}$  to  $^2\text{G}_{\text{NH}}$ , from  $^2\text{G}_{\text{NH}}$  to  $^3\text{G}_{\text{NH}}$ , and from  $^6\text{G}_{\text{NH}}$  to  $^7\text{G}_{\text{NH}}$ . Other NH-NH cross-

(15) Pajewski, R.; Ferdani, R.; Pajewska, J.; Djedovic, N.; Schlesinger, P. H.; Gokel, G. W. *Org. Biomol. Chem.* **2005**, *3*, 619–625.

(16) Pajewski, R.; Ferdani, R.; Schlesinger, P. H.; Gokel, G. W. *Chem. Commun.* **2004**, 160–1.

(17) Schlesinger, P. H.; Ferdani, R.; Pajewska, J.; Pajewski, R.; Gokel, G. W. *New J. Chem.* **2003**, *27*, 60–67.

(18) Pajewski, R.; Ferdani, R.; Gokel, G. W. *J. Am. Chem. Soc.* **2005**, *127*, JA0558894.

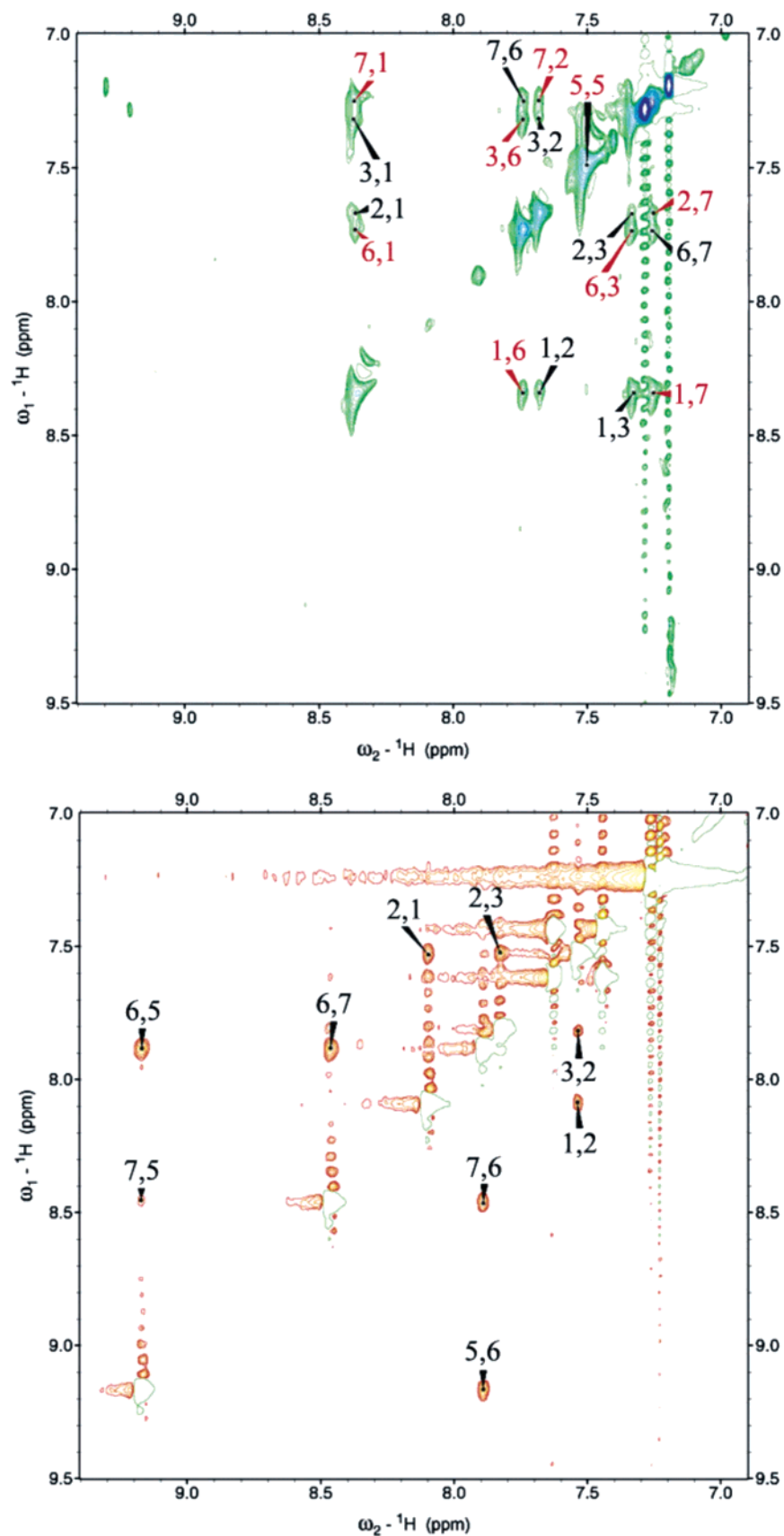


**Figure 2.** Two-dimensional  $^1\text{H}$ – $^1\text{H}$  NOESY spectra of **1** without (top) and with (bottom) tetrabutylammonium chloride. The NH–NH region is shown with cross-peaks labeled. Red labels indicate long-range connectivities. Long-range connectivities were found only in the spectra of **1** in the absence of chloride. NOESY experiments were performed in deuterated chloroform at room temperature.

peaks could be seen for  $^1\text{G}_{\text{NH}}$  to  $^3\text{G}_{\text{NH}}$ ,  $^1\text{G}_{\text{NH}}$  to  $^7\text{G}_{\text{NH}}$ ,  $^2\text{G}_{\text{NH}}$  to  $^7\text{G}_{\text{NH}}$ , and  $^3\text{G}_{\text{NH}}$  to  $^6\text{G}_{\text{NH}}$  (Figure 2, upper panel).

When  $\text{Bu}_4\text{NCl}$  was added to a solution of **1**, the following sequential residue cross-relaxations were observed:  $^1\text{G}_{\text{NH}}$  to

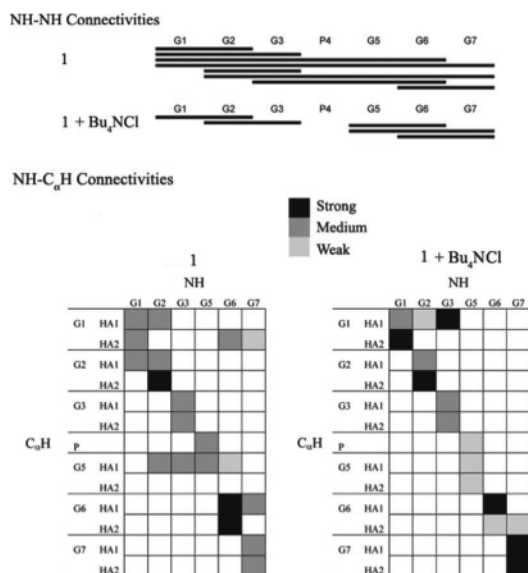


**Figure 3.** Summary of NOESY connectivities for **1** with and without Bu<sub>4</sub>NCl. NH–NH connectivities (top) are shown with a line connecting the two residues. NH–C<sub>α</sub>H connectivities (bottom) are designated weak, medium, or strong according to the intensity of the peak. HA1 and HA2 correspond to  $\alpha$ -carbon hydrogen atoms in stereochemical positions 1 and 2, respectively, as defined by the IUPAC–IUB Commission on Biochemical Nomenclature (1970).

${}^2G_{NH}$ ,  ${}^2G_{NH}$  to  ${}^3G_{NH}$ ,  ${}^5G_{NH}$  to  ${}^6G_{NH}$ , and  ${}^6G_{NH}$  to  ${}^7G_{NH}$ . Only one medium-range amide–amide interaction ( $i$ ,  $i + 2$ ) is observed ( ${}^5G_{NH}$  to  ${}^7G_{NH}$ ), and no NOE cross-peak was observed in the absence of Bu<sub>4</sub>NCl for any of the N-terminal glycines (Gly-1 to Gly-3) to amide protons of the C-terminal glycines (Gly-4 to Gly-6).

Long-range NOEs were observed for several NH–C<sub>α</sub>H interactions for **1** in the absence of Bu<sub>4</sub>NCl. Cross-peaks were apparent for  ${}^1G_{NH}$  (glycine-1 NH) to the  $\alpha$ -hydrogen of  ${}^6G$ ,  ${}^2G_{NH}$  to  ${}^5G_{C\alpha H}$ ,  ${}^3G_{NH}$  to  ${}^5G_{C\alpha H}$ ,  ${}^6G_{NH}$  to  ${}^1G_{C\alpha H}$ , and  ${}^7G_{NH}$  to  ${}^1G_{C\alpha H}$ . No long-range NOEs were observed in spectra of **1** when 10 equiv of Bu<sub>4</sub>NCl was present. Figure 3 summarizes the NOE cross-peaks that were observed in the NH–NH and NH–C<sub>α</sub>H regions. Several medium- and long-range NOEs observed for **1** in the NH–C<sub>α</sub>H region were not apparent after salt addition. The cross-peaks attributed to NH–C<sub>α</sub>H interactions nearly disappeared; no long-range but one medium-range connectivity ( ${}^3G_{NH}$  to  ${}^1G_{C\alpha H}$ ) was observed after Bu<sub>4</sub>NCl addition. Peak intensities of all assigned NOE cross-peaks in the 2D NOESY spectra were quantified to determine distance constraints. These distance constraints were then used for structure calculations.

**Circular Dichroism.** Circular dichroism (CD) spectroscopy was performed on **1** in the absence and presence of Bu<sub>4</sub>NCl (1 and 10 equiv, data not shown). A decrease in the negative absorbance intensity from 230 to 250 nm was observed upon addition of Bu<sub>4</sub>NCl, suggesting significant structural change in the presence of the ion pair. Although secondary structure information for this peptide cannot be determined from these spectra, the magnitude of the spectral changes is consistent with inferences drawn from the NMR studies described above.

**Structure Calculation and Simulation.** Structures (Figure 4) were calculated for **1** alone and in the presence of Bu<sub>4</sub>NCl using information derived from the NMR experiments (see above). Distance constraints were calculated using 35 unambiguously identified NOE peaks for the unbound and 25 peaks

for the bound heptapeptide. Of the 35 identified constraints for the unbound peptide, eight were long-range ( $i$  to  $i + >2$ ), whereas no long-range NOE constraints were considered when salt was present. The calculations were limited to the heptapeptide portion of **1** to simplify computation and because the diamine chains are expected to be unstructured in CDCl<sub>3</sub> solution. The NMR-derived structure of the peptide, shown in Figure 4, resembled a single turn of a left-handed helix. When Bu<sub>4</sub>NCl is added, the structure calculated for **1** opens up, and the C- and N-termini separate. The  $\alpha$ -carbon RMSD of the NMR structure and the final simulation structure was 0.73 Å. This separation of triglycine subunits is dictated by the lack of long-range NOEs noted above. An interesting feature of this conformation is that the amide protons of the N-terminal glycines ( ${}^5G$ – ${}^7G$ ) all reside on the same side of the peptide backbone. Glycines 5 and 7 show the largest chemical shift changes when salt is added, suggesting that this region of the peptide is in greatest proximity to chloride ion.

One way to investigate the atomic-level details of the binding process is by computer simulation.<sup>19–21</sup> A simulation of **1** in the presence of a 10-fold excess of Bu<sub>4</sub>NCl, equivalent to the NMR conditions, was performed as described in the Experimental Section. The simulation was based on the structure derived from the NMR data. After 2 ns of simulation, a single chloride ion had diffused from 12 Å away and was positioned within the cleft formed by the amide protons of the N-terminal glycines (Figure 5). This was the only high-residence-time, chloride-ion-binding event that was observed. The simulation resulted in a chloride ion within 2.31 Å of the amide hydrogen,  ${}^5G_{NH}$ , and within 2.55 Å of a second amide hydrogen,  ${}^6G_{NH}$ . The amide hydrogen,  ${}^7G_{NH}$ , was also proximate to the ion (3.12 Å), but the distance is such that asserting a definitive interaction between the two is tenuous. The chloride ion is bound to the peptide as an ion pair with tetrabutylammonium cation. This is to be expected in a low-dielectric solvent such as chloroform.

The simulation supports the experimentally determined 1:1 complexation constant,<sup>16</sup> as only a single chloride is seen interacting with the peptide for an extended period of time. These findings suggest that chloride interacts with the backbone of the heptapeptide. This apparently weak interaction accords with the requirement of both recognition and transport for **1** to function as a channel.

## Conclusions

Previous studies showed that **1** bound Bu<sub>4</sub>NCl in CDCl<sub>3</sub> with a binding constant of  $\sim 1700\text{ M}^{-1}$ . Significant shifts in the amide NMR signals were observed upon complexation. The present work confirms the previously observed changes in NMR spectra and is confirmed by CD spectra. Detailed analysis of the 2D  ${}^1H$ – ${}^1H$  TOCSY and NOESY NMR experiments accompanied by molecular simulations led to two significantly different structures for **1** in the absence and presence of Bu<sub>4</sub>NCl. An interaction between the C-terminal amide NH bonds and chloride was surmised from NMR data and is apparent in the simulations. Free **1** is helical, but the peptide is in an extended conformation in the presence of Bu<sub>4</sub>NCl. Although binding

(19) Sansom, M. S.; Adcock, C.; Smith, G. R. *J. Struct. Biol.* **1998**, *121*, 246–62.

(20) Allen, T. W.; Andersen, O. S.; Roux, B. *Proc. Natl. Acad. Sci. U.S.A.* **2004**, *101*, 117–22.

(21) Aburi, M.; Smith, P. E. *J. Phys. Chem. B* **2004**, *108*, 7382–7388.



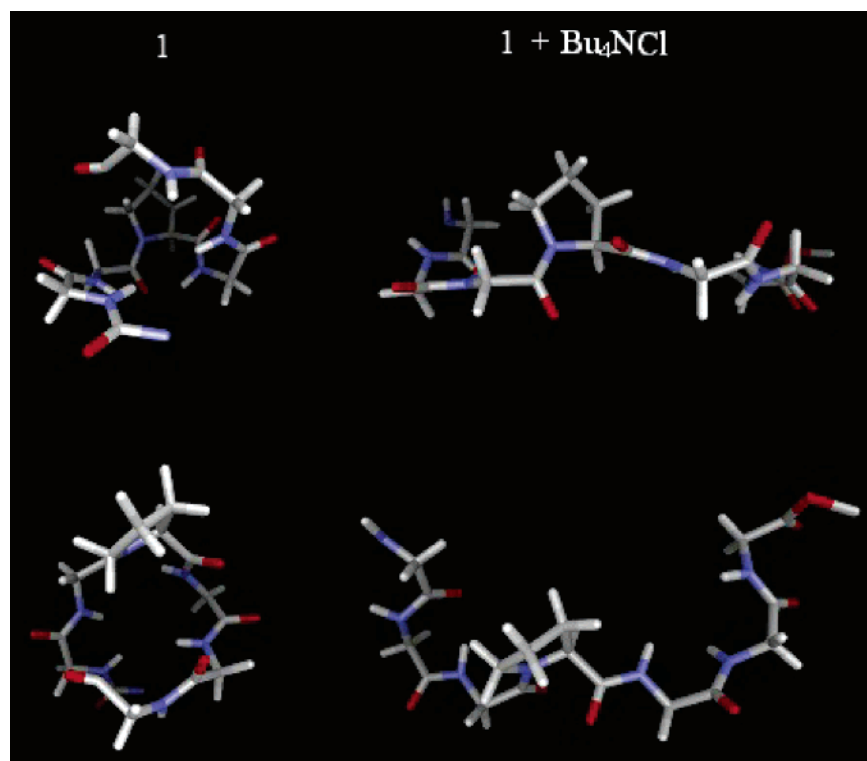


**Figure 4.** Structure of **1** in the absence (left) and presence (right) of  $\text{Bu}_4\text{NCl}$ . Structures were calculated from NOE distance constraints and  $^3J_{\alpha\text{HNH}}$  coupling-constant angle constraints. Top views of the structures are shown in the lower panel.

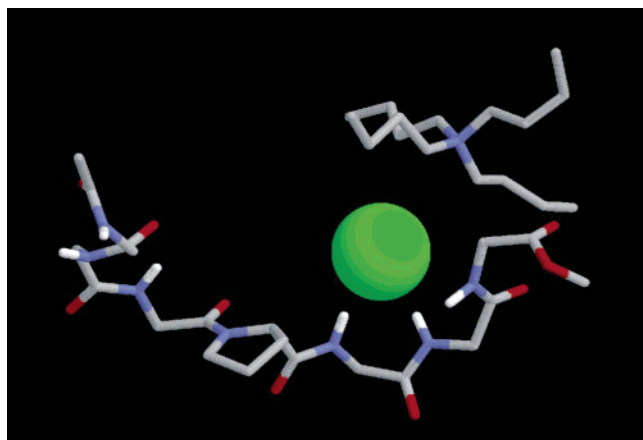


**Figure 5.** Modeled binding of  $\text{Bu}_4\text{NCl}$  to **1** in  $\text{CDCl}_3$ . The minimized structure shows two hydrogen bonds between the amide protons of glycines 5 and 6 and the chloride atom in the nondissociated salt. The chloride is shown to scale based on the van der Waals radius.

strength is highly dependent on the cation associated with chloride anion, its position was not determined by these studies. To our knowledge, this is the first detailed conformational analysis study of an active synthetic channel. The results presented here are for monomeric **1** and reference  $\text{CDCl}_3$ . The apparent interaction with chloride ion is strongly suggestive of a selectivity mechanism for this remarkable system.

## Experimental Section

**Peptide Synthesis.** Compound **1** was prepared as previously described.<sup>17</sup>

**NMR Spectroscopy.** Two-dimensional NMR spectroscopy was performed as described previously.<sup>22</sup> Briefly, all high-resolution one- and two-dimensional  $^1\text{H}$ – $^1\text{H}$  NMR experimental data were acquired with an 11.75-T Varian UNITYplus spectrometer (Varian, Palo Alto,

CA), operating at 499.96 MHz for  $^1\text{H}$ , with a 3-mm triple-resonance inverse detection probe. Using peptide concentrations of 3 mM, spectra were recorded at 25 °C in  $\text{CDCl}_3$  and were processed by Varian software VNMR 6.1c on a Sun Microsystems workstation. Standard NMR pulse sequences were used for 2D  $^1\text{H}$ – $^1\text{H}$  DQF–COSY, TOCSY, NOESY, and ROESY experiments. A total of 512 increments of 8000 data points were collected for the DQF–COSY spectra, and a total of 256 increments of 4000 data points were recorded for all other 2D NMR experiments. All data sets were obtained in hypercomplex phase-sensitive mode.

Spectra were analyzed by Sparky (T. D. Goddard and D. G. Kneller, University of California, San Francisco) on a Silicon Graphics O<sub>2</sub> workstation. Proton resonance assignments were confirmed by comparison of cross-peaks in a NOESY spectrum with those in a TOCSY spectrum<sup>23</sup> acquired under similar experimental conditions. NOESY experiments were performed with 100-, 200-, and 400-ms mixing times. ROESY spectra were acquired with a mixing time of 400 ms. TOCSY spectra were recorded using the MLEV-17 sequence<sup>24</sup> for isotropic mixing for 90 ms at a  $B_1$  field strength of 8 kHz. The chloroform peak (7.26 ppm at 25 °C) was considered as the reference for chemical shift assignments. Coupling constants ( $^3J_{\alpha\text{HNH}}$ ) were measured directly from 1D and 2D DQF–COSY<sup>25</sup> NMR spectra. All experimental data were zero-filled to 4000 data points in the  $t_1$  dimension, and when necessary, spectral resolution was enhanced by Lorentzian–Gaussian apodization.

**Structure Calculation.** The NOE spectrum of mixing time 200 ms was evaluated to provide distance constraints for the structure calculations. The volume of every unambiguously identified cross-peak was calculated within the program Sparky. These volumes were converted into inter-proton distances by setting the volume of the peak from the two  $\alpha$  protons of proline to 2.20 Å and using the program calDist (not reported). The program HABAS (Peter Güntert Scientific Software,

(22) Kirnarsky, L.; Prakash, O.; Vogen, S. M.; Nomoto, M.; Hollingsworth, M. A.; Sherman, S. *Biochemistry* **2000**, *39*, 12076–12082.

(23) Wüthrich, K. *NMR of Proteins and Nucleic Acids*; Wiley: New York, 1986.

(24) Bax, A.; Davis, D. G. *J. Magn. Reson.* **1985**, *65*, 355–360.

(25) Piantini, U.; Sorensen, O. W.; Ernst, R. R. *J. Am. Chem. Soc.* **1982**, *104*, 6800–6801.

Institute of Molecular Biology and Biophysics, Zürich, Switzerland) was used to convert coupling constant values to dihedral angle constraints. The torsion angle dynamics calculations were performed using the distance and dihedral angle constraints within the program DYANA (DYNAMics Algorithm for NMR Applications, Peter Güntert Scientific Software) on a Silicon Graphics O<sub>2</sub> workstation. The resulting 100 DYANA conformations were clustered with the software Sybyl version 6.7 (Tripos Inc., St. Louis, MO). The groups were based on the pairwise RMSD values that were less than 1-Å deviation for backbone atoms. The cluster containing the majority of the structures and lowest target function values was subjected to 100 steps of energy minimization using the Tripos force field.

**Molecular Simulations.** All molecular dynamics simulations were performed using the GROMOS96 program and the 43a1 force field.<sup>26</sup> The SPC water model<sup>27</sup> and a truncated octahedron ( $L \approx 5$  nm) were used for the simulations. Parameters for the tetrabutylammonium cations were derived using the standard rules for the GROMOS force field. The time step was 2 fs, and SHAKE<sup>28</sup> was used to constrain all bond lengths with a tolerance of  $10^{-4}$  nm. A twin-range cutoff of 0.8 nm/1.4 nm was employed, and the nonbonded pair list was updated every

5 steps. Long-range electrostatics were treated using the Poisson–Boltzmann reaction field approach,<sup>29</sup> with a reaction field permittivity for chloroform of 4.80.<sup>30</sup> The simulations were performed under conditions of constant temperature (300 K) and constant pressure (1 atm) using the weak-coupling approach.<sup>31</sup> The initial configuration for the simulation was taken from the NMR structure of **1**. This was randomly solvated with 411 chloroform molecules and 10 tetrabutylammonium chloride molecules. The system was then minimized using 1000 steps of steepest descent and simulated for 10 ns. Throughout the simulation, the peptide was restrained to the NMR-derived conformation to eliminate potential convergence problems due to the slow sampling of the large number of possible peptide conformations. Configurations were saved every 1 ps for analysis.

**Acknowledgment.** We thank the NIH for Grants GM-63190 to G.W.G., GM-74096 to J.M.T. and NSF for Grant EPS0236913 to O.P. that supported this work. This work is contribution 06-166-J from the Kansas Agricultural Experiment Station (J.M.T. and O.P.).

JA055887J

- (26) Walter, R. P. S.; Hünenberger, P. H.; Tironi, I. G.; Mark, A. E.; Billeter, S. R.; Fennen, J.; Torda, A. E.; Huber, T.; Krüger, P.; van Gunsteren, W. F. *J. Phys. Chem. A* **1999**, *103*, 3596–3607.
- (27) Berendsen, H. J. C.; Postma, J. P.; van Gunsteren, W. F.; Hemans, J. *Interaction Models for Water in Relation to Protein Hydration*; Pullman, B., Ed.; Reidel: Dordrecht, The Netherlands, 1981.
- (28) Ryckaert, J. P.; Cicotti, G.; Berendsen, H. J. C. *J. Comput. Phys.* **1977**, *23*, 327–341.

- (29) Tironi, I. G.; Sperb, R.; Smith, P. E.; van Gunsteren, W. F. *J. Chem. Phys.* **1995**, *102*, 5451–5459.
- (30) Bruno, T. J.; Svoronos, P. D. N. *CRC Handbook of Basic Tables for Chemical Analysis*; CRC Press: Boca Raton, FL, 1989.
- (31) van Gunsteren, W. F.; Berendsen, H. J. C. *Angew. Chem., Int. Ed. Engl.* **1990**, *29*, 992–1023.